Hindawi
Journal of Chemistry
Volume 2021, Article ID 5505741, 9 pages
https://doi.org/10.1155/2021/5505741

*Research Article*

# Antioxidative Reactivity of L-Ascorbic Acid and D-Isoascorbic Acid Species towards Reduction of Hexachloroiridate (IV)

**Han Zhang,[1] Yanqing Xia,[1] Peng Zhang,[2] Liqian Hou,[1] Ying Sun,[3] Zhaozhan Lu,[3] Yunfeng Tang,[3] Hongwu Tian,[3] and Tiesheng Shi[1]**

[1]*College of Chemistry, Chemical Engineering, and Materials Science, Zaozhuang University, Zaozhuang 277160, Shandong Province, China*
[2]*Department of Articular Surgery, Linyi People's Hospital, Linyi 276100, Shandong Province, China*
[3]*National Engineering Technology Center of Chirality Pharmaceuticals, Lunan Pharmaceutical Group Co.,Ltd., Linyi 276006, Shandong Province, China*

Correspondence should be addressed to Tiesheng Shi; rock@uzz.edu.cn

Received 20 July 2021; Revised 28 October 2021; Accepted 30 October 2021; Published 18 November 2021

Academic Editor: Cláudia G. Silva



The pair $[IrCl_6]^{2-}/[IrCl_6]^{3-}$ has been demonstrated to be a good redox probe in biological systems while L-ascorbic acid (AA) is one of the most important antioxidants. D-isoascorbic acid (IAA) is an epimer of AA and is widely used as an antioxidant in various foods, beverages, meat, and fisher products. Reductions of $[IrCl_6]^{2-}$ by AA and IAA have been analyzed kinetically and mechanistically in this work. The reductions strictly follow overall second-order kinetics and the observed second-order rate constants were collected in the pH region of $0 \le pH \le 2.33$ at 25.0°C. Spectrophotometric titration experiments revealed a well-defined 1 : 2 stoichiometry, namely $\Delta[AA] : \Delta[Ir(IV)]$ or $\Delta[IAA] : \Delta[Ir(IV)] = 1 : 2$, indicating that L-dehydroascorbic acid (DHA) and D-dehydroisoascorbic acid (DHIA) were the oxidation products of AA and IAA, respectively. A reaction mechanism is suggested involving parallel reactions of $[IrCl_6]^{2-}$ with three protolysis species of AA/IAA (fully protonated, monoanionic, and dianionic forms) as the rate-determining steps and formation of ascorbic/isoascorbic and ascorbate/isoascorbate radicals; in each of the steps, $[IrCl_6]^{2-}$ acquires an electron via an outer-sphere electron transfer mode. Rate constants of the rate-determining steps have been derived or estimated. The fully protonated forms of AA and IAA display virtually identical reactivity whereas ascorbate and isoascorbate monoanions have a significant reactivity difference. The ascorbate and isoascorbate dianions are extremely reactive and their reactions with $[IrCl_6]^{2-}$ proceed with the diffusion-controlled rate. The species versus pH and the species reactivity versus pH distribution diagrams were constructed endowing that the ascorbate/isoascorbate monoanionic form dominated the total reactivity at physiological pH. In addition, the value of $pK_{a1} = 3.74 \pm 0.05$ for IAA at 25.0°C and 1.0 M ionic strength was determined in this work.

## 1. Introduction

Vitamin C is a general name for all the compounds which possess the fully or partially biological activity of L-ascorbic acid (AA) [1–6]. It includes AA itself, L-dehydroascorbic acid (DHA), the esters of AA such as ascorbyl palmitate, and D-isoascorbic acid (IAA); the latter two are the synthetic compounds [1–3]. Vitamin C is widely found in plants (vegetables and fruits in particular) and in animals, and nowadays it is also available as caplets, tablets, capsules, and drink mixes and in multivitamin and antioxidant formulations [1–3]. Biologically and/or medically, extensive investigations of vitamin C have been carried out [7, 8]. When vitamin C is utilized in food and nutrients, its antioxidative property is often considered to be an important factor [9, 10]. IAA is an epimer of AA and widely used as an antioxidant in various foods, beverages, meat, and fisher products [2, 11–15]. In this regard, several analytical methods have been developed to determine content of IAA in foodstuffs, together with those

of AA and their oxidized forms [2, 11–15]. Scheme 1 provides the structures of AA, IAA and their oxidized forms.

As one of the most important antioxidants, the kinetics and mechanisms of vitamin C/ascorbic acid reactions with various oxidants have been explored extensively [9, 10, 16–20]; the oxidants include reactive oxygen species such as $HO_2/O_2^-$ radicals and peroxynitrite, and some metal ions/complexes [16–19]. Among the metal ions/complexes, single electron oxidants apparently dominate the exploration [9, 10]. We have had an interest in the study of the redox pair $[IrCl_6]^{2-}/[IrCl_6]^{3-}$ due to its salient characters: (i) $[IrCl_6]^{2-}$ has two strong absorption bands (around 420 and 488 nm, vide infra) and $[IrCl_6]^{3-}$ does not possess these two bands, conferring a convenient monitoring of the pair. (ii) $[IrCl_6]^{2-}$ is very stable and meta-stable from pH 0 to 10, enabling us to measure the rate constants in such a wide pH range [20–22]. (iii) It has been used as a redox probe to discriminate DNA monolayers and to obtain chemical information of oxidative stress in biological matrixes [23, 24].

The antioxidative reactivity of AA and IAA towards reduction of $[IrCl_6]^{2-}$ has been investigated in this work. Previously, the kinetics of oxidation of AA by $[IrCl_6]^{2-}$ was studied [25, 26], but only was carried out in a very narrow acidity region (namely, $0.20\,M \le [HClO_4] \le 1.00\,M$). On the other hand, the redox reaction between $[IrCl_6]^{2-}$ and IAA has never been investigated. In fact, the oxidation kinetic and mechanistic aspects of the IAA oxidations were poorly understood due to a very limited study [19]. The purposes of the present work were to study the redox reactions in a pH range as wide as possible, to derive the rate constants of the rate-determining steps in a good accuracy, to propose a convincing reaction mechanism, and to find out the antioxidative difference between AA and IAA.

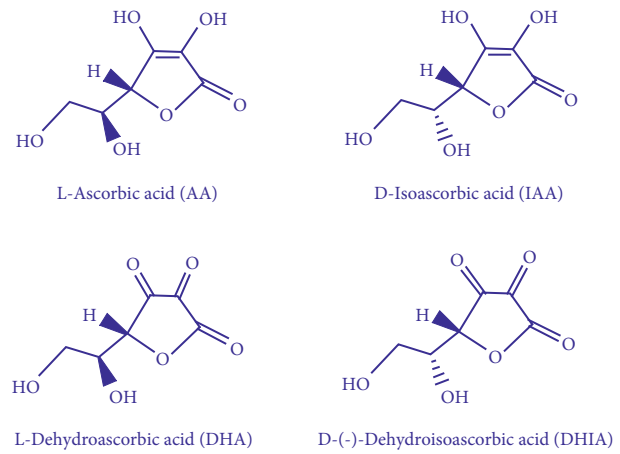


Scheme 1: Structures of L-ascorbic acid and D-isoascorbic acid and of their common oxidation forms L-dehydroascorbic acid and D-dehydroisoascorbic acid.

## 2. Experimental Section

*2.1. Materials.* Sodium hexachloroiridate(IV) hexahydrate ($Na_2IrCl_6{\cdot}6H_2O$, 99.9%) and L-ascorbic acid (AA, 99%) were purchased from Sigma-Aldrich. D-(-)-isoascorbic acid (IAA, HPLC grade, purity ≥99%) was obtained in its purest form from Yuanye Biological Company (Shanghai, China). Concentrated perchloric acid, sodium perchlorate monohydrate, concentrated *o*-phosphoric acid (ca. 85%), sodium dihydrogen-phosphate, disodium hydrogen phosphate, acetic acid, sodium acetate, sodium chloride, and 0.100 M NaOH standard solution were purchased in the purest forms available either from Fisher Scientific (Fisher Scientific, Shanghai, China) or from Alfa Aesar (Alfa Aesar Branch in Shanghai, China). These chemicals were used directly without further purification. For pH meter calibrations, standard buffers of pH 4.00, 7.00, and 10.00 were purchased from ThermoFisher. Doubly distilled water was used throughout this work.

*2.2. Reaction Media or Buffer Solutions.* Stock solutions of 1.00 M $HClO_4$ and $H_3PO_4$ were prepared from the concentrated acids and standardized by the 0.100 M NaOH solution. For $pH \le 2.11$, the reaction media were prepared by combinations of the 1.00 M $HClO_4$ with 1.00 M $NaClO_4$; their pH values were derived by use of the equation: $pH = -\log[H^+] + 0.11$, which is based on a mean activity coefficient of 0.77 in solutions of 1.00 M $NaClO_4$ [27]. For buffer solutions in the pH range from 2.28 to 6.26, the combinations of the buffering pairs $H_3PO_4/NaH_2PO_4$, AcOH/NaOAc, and $NaH_2PO_4/Na_2HPO_4$ (0.15–0.2 M) were employed. All the buffers were tuned to an ionic strength of 1.0 M by use of $NaClO_4{\cdot}H_2O$; their pH values were measured by an Accumet Basic AB150 Plus pH meter, equipped with an Accumet accuTupH® combination pH electrode (ThermoFisher). The electrode was calibrated using standard buffers of pH 4.00, 7.00, and 10.00 immediately before pH measurements. These buffer solutions were only used weekly.

*2.3. Kinetic Experiments.* Stock solutions of about 10 mM $[IrCl_6]^{2-}$ were prepared daily by dissolving the desired amount of $Na_2IrCl_6{\cdot}6H_2O$ in a solution containing 0.90 M $NaClO_4$, 0.09 M NaCl, and 0.01 M HCl; these solutions were only used daily. Stock solutions of AA/IAA were prepared by adding the desired amount of AA/IAA to a buffer solution of specific pH. Each of the solutions was bubbled with pure nitrogen for 5 min and was only employed for ca. 2 h. Solutions of $[IrCl_6]^{2-}$ and AA/IAA for kinetic measurements were made by dilution of the above stock solutions with the same pH buffer; these solutions were loaded onto an Applied Photophysics SX-20 stopped-flow spectrometer (Applied Photophysics Ltd., Leatherhead, UK). A water bath circulation from a thermostat (Lauda Alpha RA8, Delran, NJ, USA) was employed for the temperature control at $25.0 \pm 0.1$°C. Kinetic traces were recorded by mixing equal volumes of the $[IrCl_6]^{2-}$ and AA/IAA solutions directly in the stopped-flow spectrometer. Pseudo-first-order conditions (namely, $[AA]_{tot}$ or $[IAA]_{tot} \ge 10 \bullet [Ir(IV)]$) were always maintained, where $[AA]_{tot}$ and $[IAA]_{tot}$ are ascribed to the total concentrations of AA and IAA, respectively.

*2.4. Spectrophotometric Titration Experiments.* UV-Vis spectra were recorded on a TU-1900 spectrophotometer by use of 1.00 cm quartz cells at 25.0°C (Beijing Persee, Beijing, China); the temperature was controlled by a water circulation from the same type of thermostat. There were series of reaction mixtures in which [Ir(IV)] = 0.40 mM was kept unchanged and $[AA]_{tot}/[IAA]_{tot}$ was varied from 0 to 0.50 mM in a reaction medium of $[H^+]$ = 0.10 M and 1.0 M ionic strength. Each of the reaction mixtures was controlled at 25°C for about 5 min; the absorption value was measured at 488 nm.

## 3. Results and Discussion

*3.1. Spectral Insight into the Reaction Courses.* Although an outer-sphere electron transfer was suggested for the oxidation of AA by $[IrCl_6]^{2-}$, the reaction course was not exploited previously [25, 26]. The rapid scan spectra were thus recorded for the oxidations of AA/IAA by $[IrCl_6]^{2-}$ in this work; Figure 1 displays such spectra in the case of AA. Clearly the absorption bands around 488, 420, and 306 nm, which are the typical ones of $[IrCl_6]^{2-}$, remained upshifted; in addition, no new absorption bands emerged during the reaction course. Moreover, the kinetic traces recorded at these bands could be well described by single exponentials, giving rise to the values of pseudo-first-order constants $k_{obsd}$. The above reaction characters indicate that a simple electron transfer took place without complications such as an adduct formation or faster substitution reactions on $[IrCl_6]^{2-}$ before the rate-determining step(s). It is thus concluded that the redox reaction is indeed first-order in [Ir(IV)]. The rapid scan spectra in the case of IAA are very similar to those shown in Figure 1.

*3.2. Second-Order Kinetics.* Still under pseudo-first-order conditions, the reaction rates were determined when $[AA]_{tot}/[IAA]_{tot}$ was varied in the region $0.10 \le [AA]_{tot}/[IAA]_{tot} \le 2.0$ mM; for this concentration region, the reaction media had enough buffering capacities to ascertain that no pH changes could be caused by the variations of the concentrations of the reductants. The values of $k_{obsd}$ as functions of $[AA]_{tot}$ or $[IAA]_{tot}$ and of pH were collected; for each concentration, the $k_{obsd}$ value is reported as an average of the at least 5 duplicate runs and the standard deviations were usually less than 5%. Plots of $k_{obsd}$ versus $[AA]_{tot}$ are displayed in Figure 2 and versus $[IAA]_{tot}$ are shown in Figure 3; undoubtedly the linearity of the plots is very good, and no significant intercepts are observable. Hence, the redox reactions are first-order in $[AA]_{tot}$ or $[IAA]_{tot}$, rendering overall second-order kinetics as described by equations (1a) and (1b), where $k'$ stands for the observed second-order rate constants.

$$-\frac{d[\mathrm{Ir(IV)}]}{dt} = k'[AA]_{tot}[\mathrm{Ir(IV)}], \quad (1a)$$

$$-\frac{d[\mathrm{Ir(IV)}]}{dt} = k'[IAA]_{tot}[\mathrm{Ir(IV)}]. \quad (1b)$$

Values of $k'$ were calculated from the plots in Figures 2 and 3 and are summarized in Table 1. In addition, plots of

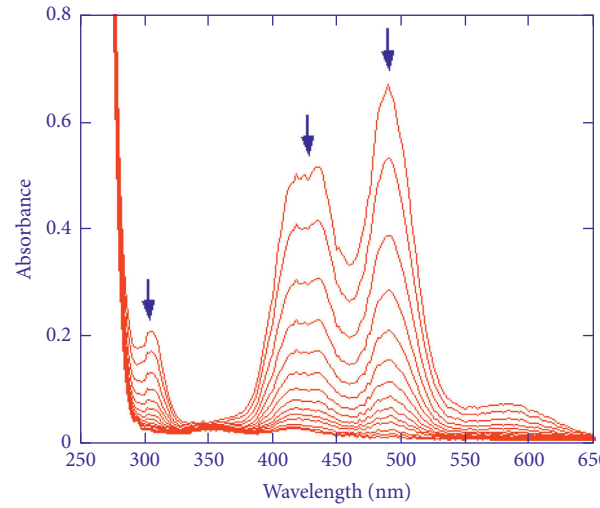


Figure 1: Rapid scan spectra for reduction of $[IrCl_6]^{2-}$ by L-ascorbic acid (AA). Reaction conditions: [Ir(IV)] = 0.20 mM, $[AA]_{tot}$ = 2.00 mM, $[H^+]$ = 0.200 M, $\mu$ = 1.0 M, temperature of 25.0°C. The spectra were acquired at 2, 5, 10, 15, 20, 25, 30, 35, 40, 45, 50, 60, 70, and 80 milliseconds (ms) after mixing.

log$k'$ versus pH are shown in Figure 4 (data points). The stopped-flow spectrometer was employed essentially to its up limit for following the redox reactions.

*3.3. The Reaction Stoichiometry.* The stoichiometric ratios were determined in a medium of 0.10 M $HClO_4$ and 0.90 M $NaClO_4$ by use of spectrophotometric titration method which was demonstrated to be a very useful approach [28–31]. The absorption values at 488 nm as a function of $[AA]_{tot}$ or $[IAA]_{tot}$ are shown in Figure 5; in either case, the data points all follow two crossing straight lines. The intersection points in Figure 5 confer stoichiometric ratios: $\Delta[\mathrm{Ir(IV)}] : \Delta[AA]_{tot} = 0.40\ \mathrm{mM} : 0.202\ \mathrm{mM} = 1 : (0.51 \pm 0.01)$ and $\Delta[\mathrm{Ir(IV)}] : \Delta[IAA]_{tot} = 0.40\ \mathrm{mM} : 0.196\ \mathrm{mM} = 1 : (0.49 \pm 0.01)$. Thus, the derived stoichiometric ratios $\Delta[AA]_{tot} : \Delta[\mathrm{Ir(IV)}]$ and $\Delta[IAA]_{tot} : \Delta[\mathrm{Ir(IV)}] = 1 : 2$ are established unambiguously when the experimental errors are considered. This is perhaps not surprising because commonly AA is oxidized to DHA and IAA is oxidized to D-dehydroisoascorbic acid (DHIA), *cf.* structures in Scheme 1. The stoichiometric reactions in the present reaction systems can be expressed by

$$2[IrCl_6]^{2-} + AA \longrightarrow 2[IrCl_6]^{3-} + DHA + 2H^+ \quad (2a)$$

$$2[IrCl_6]^{2-} + IAA \longrightarrow 2[IrCl_6]^{3-} + DHIA + 2H^+ \quad (2b)$$

*3.4. Acid Dissociation Constants of AA and IAA.* Acid dissociation constants of AA were reported to be $pK_{a1} = 3.96$ [32] and $pK_{a2} = 11.24$ [27] at 25.0°C and 1.0 M ionic strength. A value of $pK_{a1} = 2.706$ for IAA was reported in solutions of 0.16 M NaCl at 25.0°C [19]; in order to match the reaction conditions used in this work, this value was determined spectrophotometrically in this work at 25.0°C and 1.0 M

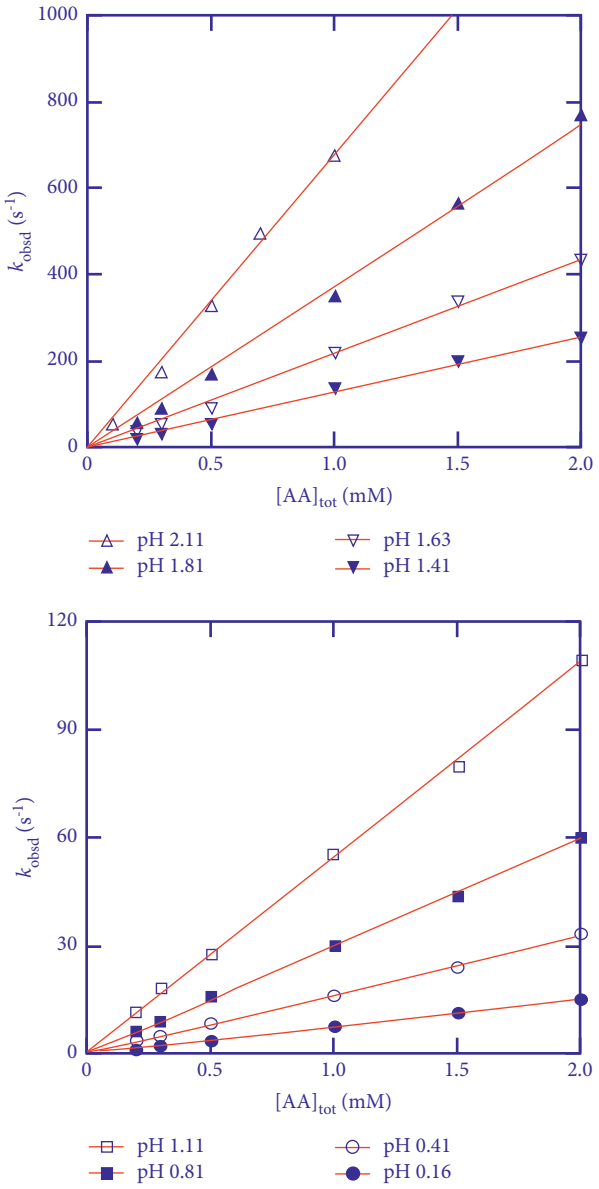


FIGURE 2: Dependencies of $k_{obsd}$ on $[AA]_{tot}$ at 25.0°C and 1.0 M ionic strength for reduction of $[IrCl_6]^{2-}$ by AA.

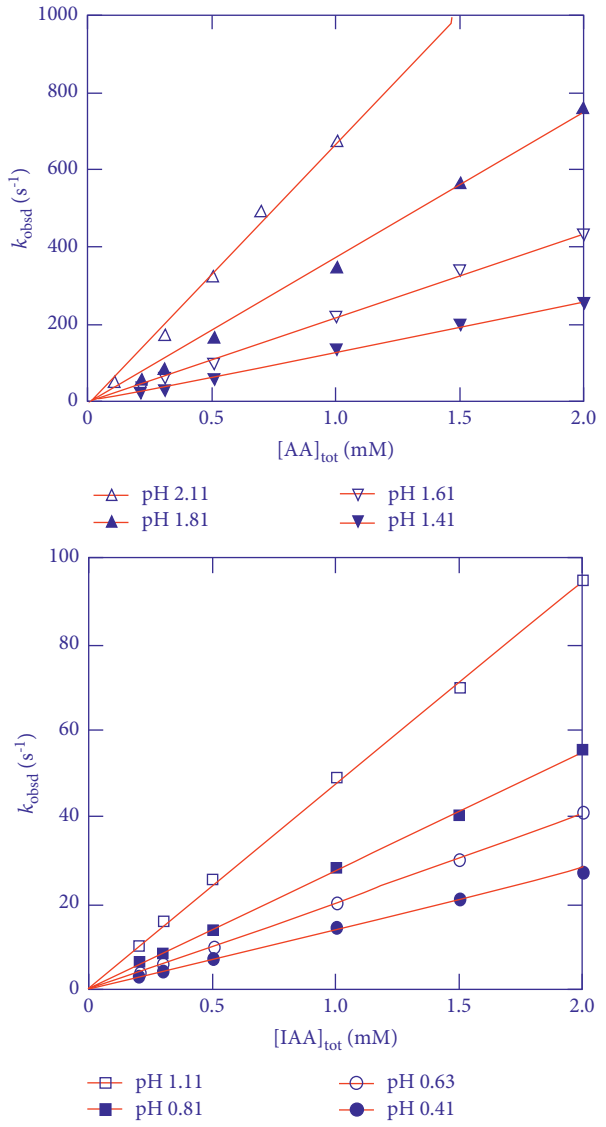


FIGURE 3: Dependencies of $k_{obsd}$ on $[IAA]_{tot}$ at 25.0°C and 1.0 M ionic strength for reduction of $[IrCl_6]^{2-}$ by IAA.

ionic strength. UV-Vis spectra were recorded for 0.10 mM IAA in a series of buffer solutions covering a pH range from 2.28 to 6.26; before recording each spectrum, a fresh IAA solution and the corresponding buffer solution as reference were thermoequilibrated at 25.0°C for about 10 min. The spectra recorded in pH 2.28, 3.89, and 6.26 buffers are given in the upper panel of Figure 6; an rough isosbestic point in the figure indicates two absorbing species are present. The wavelength of 266 nm was then chosen for the measurements of absorption values. The measured values as a function of pH are given in the lower panel of Figure 6 (data points). Equation (3) was utilized to simulate the data by use of a nonlinear least-squares method [29, 30], where $\varepsilon_1$ and $\varepsilon_2$ pertain to the molar absorptivities of fully protonated and monoanionic forms of IAA, respectively.

$$\text{Abs}\,(266\,\text{nm}) = [\text{IAA}]_{\text{tot}} \frac{\left\{\varepsilon_2 + \varepsilon_1 \cdot 10^{\left(\text{pK}_{a_1} - \text{pH}\right)}\right\}}{\left\{1 + 10^{\left(\text{pK}_{a_1} - \text{pH}\right)}\right\}}. \quad (3)$$

The simulation confers a good fit (*cf.* the lower panel of Figure 6) and affords $pK_{a1} = 3.74 \pm 0.05$ at 25.0°C and 1.0 M ionic strength; this value is virtually identical to that reported earlier albeit with a difference in ionic strength [19]. Since the $pK_{a2}$ value was expected to be very close to that of AA and far from the pH region used in this work, we did not determine it.

*3.5. Reaction Mechanism.* The observed second-order rate constants in Table 1 increased more than 100 times when pH was changed from 0.16 to 2.33 for both AA and IAA, indicating that their monoanionic forms have a much higher reactivity than the fully protonated forms. The increasing trends are anticipated to continue, but the reactions became too fast to

Table 1: Observed second-order rate constants for the reduction of $[IrCl_6]^{2-}$ by AA and IAA at 25.0°C and 1.0 M ionic strength.

| Reductant | pH | $k'/M^{-1}s^{-1}$ |
|---|---|---|
| AA | 0.16 | $(7.6 \pm 0.1) \times 10^3$ |
| | 0.26 | $(9.6 \pm 0.2) \times 10^3$ |
| | 0.41 | $(1.66 \pm 0.02) \times 10^4$ |
| | 0.63 | $(2.42 \pm 0.04) \times 10^4$ |
| | 0.81 | $(3.01 \pm 0.06) \times 10^4$ |
| | 1.11 | $(5.49 \pm 0.09) \times 10^4$ |
| | 1.41 | $(1.29 \pm 0.03) \times 10^5$ |
| | 1.63 | $(2.19 \pm 0.05) \times 10^5$ |
| | 1.81 | $(3.75 \pm 0.09) \times 10^5$ |
| | 2.11 | $(6.8 \pm 0.2) \times 10^5$ |
| | 2.33 | $(1.15 \pm 0.06) \times 10^6$ |
| IAA | 0.16 | $(7.5 \pm 0.1) \times 10^3$ |
| | 0.26 | $(8.3 \pm 0.2) \times 10^3$ |
| | 0.41 | $(1.40 \pm 0.02) \times 10^4$ |
| | 0.63 | $(2.04 \pm 0.04) \times 10^4$ |
| | 0.81 | $(2.78 \pm 0.06) \times 10^4$ |
| | 1.11 | $(4.78 \pm 0.08) \times 10^4$ |
| | 1.41 | $(9.4 \pm 0.03) \times 10^4$ |
| | 1.63 | $(1.97 \pm 0.04) \times 10^5$ |
| | 1.81 | $(3.10 \pm 0.07) \times 10^5$ |
| | 2.11 | $(6.1 \pm 0.1) \times 10^5$ |
| | 2.33 | $(1.00 \pm 0.02) \times 10^6$ |

follow by the stopped-flow spectrometer when pH > 2.33. In analogy, the fully deprotonated species of AA and IAA are anticipated to have the highest reactivity among their 3 protolysis species [17]. Since the attributes of the rapid scan spectra suggest that the electron transfer reactions between $[IrCl_6]^{2-}$ and AA/IAA undergo directly, it is logical to assume that all the protolysis species of AA/IAA in Scheme 2 will reduce $[IrCl_6]^{2-}$. A reaction mechanism is proposed as delineated in Scheme 2 which involves the three protolysis species of AA/IAA reacting with $[IrCl_6]^{2-}$ in parallel; the parallel reactions as indicated by $k_1$-$k_3$ are the rate-determining steps. In each of the rate-determining steps, a single electron transfer takes place, generating a free radical species. Thus, three different free radicals as highly reactive transients are likely involved in the mechanism, *cf.* the possible structures of the free radicals in Scheme 2 [9, 10, 33]. Each of the free radicals is reacting with another $[IrCl_6]^{2-}$ in subsequently fast reaction leading to formation of DHA or DHIA.

*3.6. Evaluation of the Rate Constants.* The rate law of equation (4) can be derived from the reaction mechanism in Scheme 2 in the case of AA, where $a_H$ denotes the proton activity corresponding to the pH measurements and the factor 2 in the equation comes from the stoichiometric ratio, *cf.* equations (2a) and (2b). For the reaction of IAA, the rate law is identical except that $[IAA]_{tot}$ replaces $[IAA]_{tot}$ in

$$-\frac{d\left[IrCl_6^{2-}\right]}{dt} = \frac{2\left(k_1 a_H^2 + k_2 K_{a1} a_H + k_3 K_{a_1} K_{a_2}\right)}{a_H^2 + K_{a1} a_H + K_{a_1} K_{a_2}} [AA]_{tot} \left[IrCl_6^{2-}\right]. \quad (4)$$

When equation (4) is compared with equation (1a), it confers the expression of $k'$:

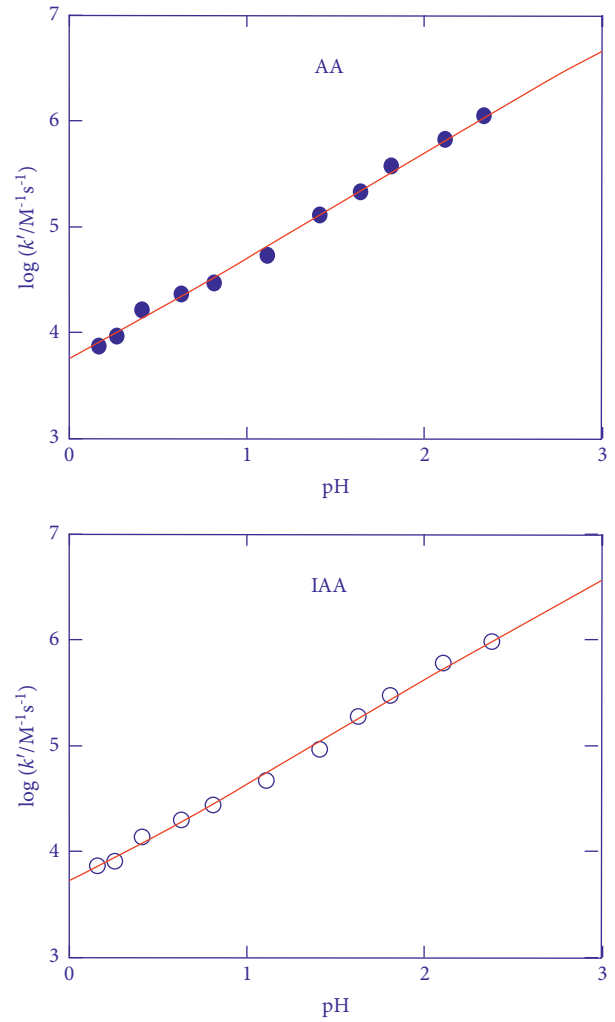


Figure 4: Second-order rate constants $k'$ (in logarithmic scale) versus pH plots at 25.0°C and 1.0 M ionic strength (data points) for reduction of $[IrCl_6]^{2-}$ by AA and IAA. The solid lines represent the best fits of equation (6) to the experimental data by use of a weighted nonlinear least-squares method.

$$k' = \frac{2\left(k_1 a_H^2 + k_2 K_{a1} a_H + k_3 K_{a_1} K_{a_2}\right)}{a_H^2 + K_{a1} a_H + K_{a_1} K_{a_2}}. \quad (5)$$

Equation (5) was used to simulate the $k'$-pH dependence data by use of a weighted nonlinear least-squares method [34]. In the simulation of the AA reaction, $pK_{a1} = 3.96$ and $pK_{a2} = 11.24$ were used as direct inputs and $k_1$, $k_2$, and $k_3$ were treated as tunable parameters. The simulation resulted in a set of values ($k_1 = 611 \pm 67\ M^{-1}s^{-1}$, $k_2 = 2.2 \times 10^7\ M^{-1}s^{-1}$, and $k_3 = 3.3 \times 10^{15}\ M^{-1}s^{-1}$); however, the value of $k_3$ is over the diffusion-controlled rate constant (ca. $10^{10}\ M^{-1}s^{-1}$ in aqueous solution) [35]. Since the $k_2 >> k_1$, the $k_3$ value is expected to be also several orders of magnitude higher than $k_2$ [17]. It is thus reasonable to assume that $k_3$ takes a diffusion-controlled rate constant [35]. Given an assumption that $k_3 = 10^{10}\ M^{-1}s^{-1}$, the simulation was executed again and the simulated resulted is shown in the upper panel of Figure 4, concurrently providing $k_1 = 451 \pm 59\ M^{-1}s^{-1}$ and

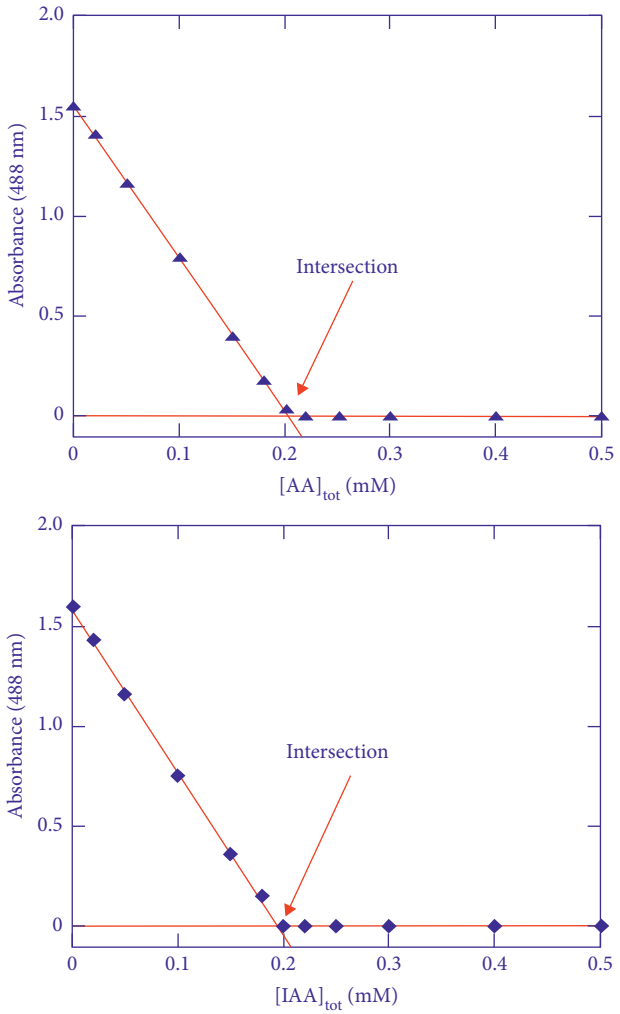


Figure 5: Determination of the reaction stoichiometries by spectrophotometric titrations for reduction of $[IrCl_6]^{2-}$ by AA and IAA. Absorbance at 488 nm versus $[AA]_{tot}$ or $[IAA]_{tot}$ for a series of reaction mixtures in which [Ir(IV)] = 0.40 mM kept constant and $[AA]_{tot}$ or $[IAA]_{tot}$ varied from 0 to 0.50 mM. Reaction medium: $[H^+]$ = 0.10 M and 1.0 M ionic strength; reaction time is about 5 min, room temperature.

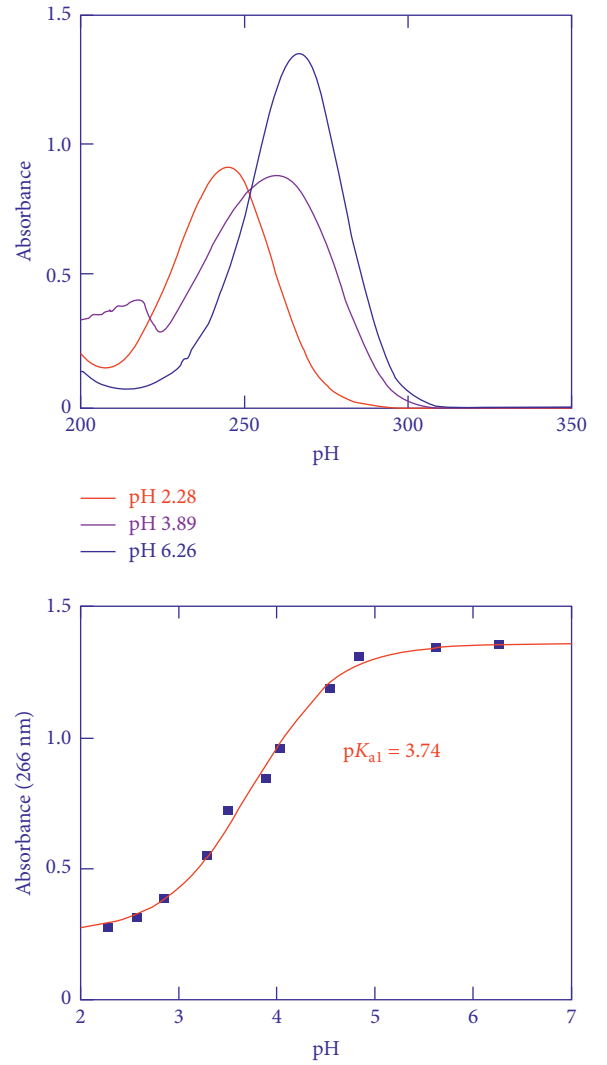


Figure 6: (a) Electronic spectra recorded for 0.10 mM IAA in three different buffer solutions of 1.0 M ionic strength at 25.0°C. (b) Absorption values at 266 nm of 0.10 mM IAA solutions as a function of pH at 25.0°C (data points). The solid line was obtained from the best fit of equation (3) to experimental data by use of a nonlinear least-squares method.

$k_2 = (2.28 \pm 005)\ x\ 10^7\ M^{-1}s^{-1}$. Alternatively, if the $k_3$-term in equation (5) is neglected, equation (5) is simplified to

$$k' = \frac{2\left(k_1 a_H + k_2 K_{a1}\right)}{a_H + K_{a1}}. \quad (6)$$

When equation (6) was utilized to simulate the data, an identical fit and identical values of $k_1$ and $k_2$ were obtained (Table 2), indicating that even $k_3$ takes a diffusion-controlled rate constant; the contribution from ascorbate dianion in the pH region used in this work is negligible. This is understandable because the $pK_{a2}$ value of AA is far from the pH region studied. Nevertheless, a well-defined $k_2$ value is obtained.

For the reaction of IAA, the above simulations were also performed and the simulated results were very similar. Consequently, the simulation of the $k'$-pH dependence data by equation (6) confers an excellent fit (the lower panel of Figure 4) by use of $pK_{a1} = 3.74$ determined in this work; the values of $k_1$ and $k_2$ acquired from the fit are listed in Table 2. For both AA and IAA, the relatively large errors associated with $k_1$ values are ascribed to the much higher values of $k_2$, which dominates the total reactivity in the pH region studied.

The oxidation kinetics of ascorbic acid by $[IrCl_6]^{2-}$ was studied only in a narrow acidity region ($0.20\ M \le [HClO_4] \le 1.00\ M$); the derived rate constants were $k_1 < 200\ M^{-1}s^{-1}$ and $k_2 = 1.4 \times 10^7\ M^{-1}s^{-1}$ at 20.0°C and 1.0 M ionic strength from this region (a correction of a stoichiometric factor was made) [25]. These values were not well determined due to the very narrow acidity region used and are significantly smaller than those obtained in this work; our values derived from a much wider pH region are more accurate and of course more

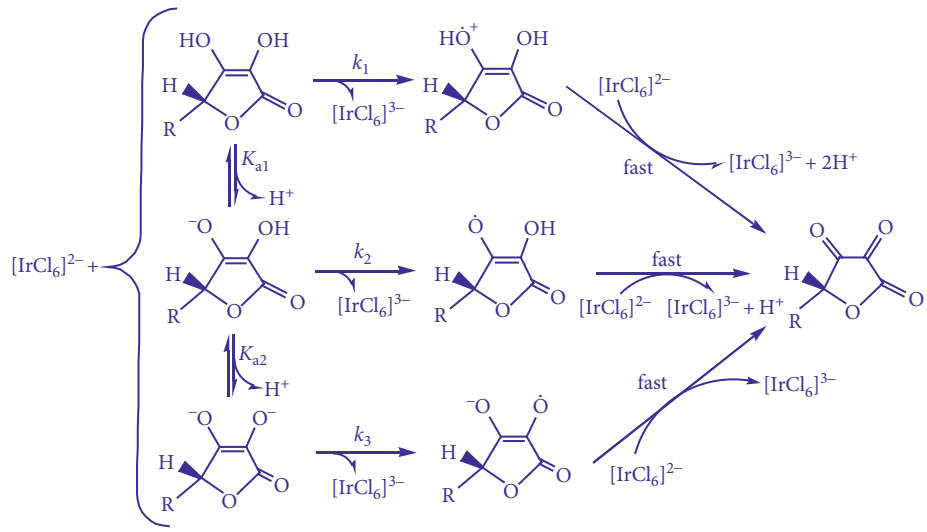


Scheme 2: Schematically deciphering the reaction mechanism for reduction of $[IrCl_6]^{2-}$ by L-ascorbic acid and D-isoascorbic acid (R represents the side chains of AA and IAA, *cf.* Scheme 1).

Table 2: Rate constants for the rate-determining steps at 25.0°C and 1.0 M ionic strength.

| Reductant | $k_m$ | Values ($M^{-1}s^{-1}$) |
|---|---|---|
| AA | $k_1$ | $451 \pm 59$ |
| | $k_2$ | $(2.28 \pm 0.05) \times 10^7$ |
| | $k_3$ | Diffusion controlled |
| IAA | $k_1$ | $487 \pm 45$ |
| | $k_2$ | $(1.19 \pm 0.03) \times 10^7$ |
| | $k_3$ | Diffusion controlled |

reliable. Moreover, the $k_3$ value is estimated to be a rate constant of the diffusion-controlled one in aqueous solution.

*3.7. Antioxidative Reactivity of the AA and IAA Species.* The acquired $k_1$ and $k_2$ values for IAA provide a direct comparison with AA. While the $k_1$ values are essentially identical within the experimental errors, the $k_2$ values have a clear difference, namely $k_2$ (AA) $\approx 2k_2$ (IAA); this reactivity difference is ascribed probably to the slightly lower p$K_{a1}$ value of IAA. The reactivity difference suggests that the antioxidative power of IAA is weaker than that of AA in the acidic to neutral media where the ascorbate monoanions dominate their respective populations (vide infra).

For both AA and IAA, the kinetic characters observed in the present work bolster the conclusion that the redox reactions take place via an outer sphere electron-transfer mode [25, 26]. It is clearly shown from the data in Table 2 that $k_1 << k_2 << k_3$. In a more visualized way, the species population versus pH distribution diagram and the species reactivity versus pH distribution diagram were contrarily constructed for the AA reaction [36], which are displayed in Figure 7 (the diagrams for the IAA reaction are very similar and are not shown). A few attributes are discerned from the diagrams: (a) the fully protonated AA exists between pH 0 and 6, but it only contributes slightly to the total reactivity in

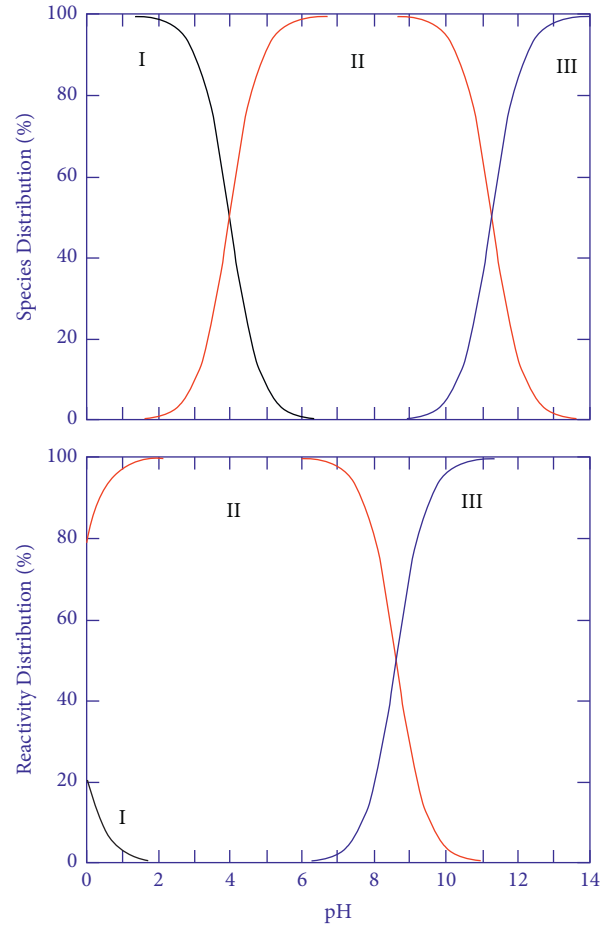


Figure 7: (a) Species of AA versus pH distribution diagram (*cf.* Scheme 2). (b) Reactivity of AA species versus pH diagram computed by use of $k_1 = 451\ M^{-1}s^{-1}$, $k_2 = 2.28 \times 10^7\ M^{-1}s^{-1}$ and $k_3 = 1 \times 10^{10}\ M^{-1}s^{-1}$ (a diffusion-controlled rate constant in aqueous solution). (I) Fully protonated form of AA; (II) monoanionic form of AA; (III) dianionic form of AA.

an acidic region (pH from 0 to 2). (b) At the biological matrix of pH 7.0–7.4, the ascorbate monoanion dominates both the species population and the total reactivity. (c) The ascorbate dianion exists only in basic media (pH > 10), but it comes into play as early as pH 6.5 and takes a leading role when pH > 9. The reactivity of AA/IAA species toward reductions of single electron oxidants involved in our body may show similar characters observed above. The significance of the above analysis is that when AA and IAA are used as additives in foods and drinks, these foods and drinks will pass through our digestive systems, where stomach and intestines are in frontlines possessing an acidic environment (pH range from 2 to 5), and the monoanionic forms of AA and IAA may take a leading role in reductions of free radicals or single electron oxidants. Consequently, the antioxidative reactivity of IAA is only about half that of AA.

## 4. Conclusions

The reduction reactions of $[IrCl_6]^{2-}$ by AA and IAA have been analyzed kinetically and mechanistically by use of rapid scan and stopped-flow spectral techniques. The reactions strictly follow overall second-order kinetics. The proposed reaction mechanism involves three parallel reactions being the rate-determining steps; in each of the reactions $[IrCl_6]^{2-}$ acquires an electron via an outer-sphere electron transfer mode. Rate constants of the rate-determining steps have been derived or estimated which are confidently reliable. A direct comparison between reactivity of AA and IAA demonstrates that IAA has about a half antioxidative reactivity of that of AA in slightly acidic to neutral media. The antioxidative data acquired for AA and IAA can be used as a reference for comparisons with other biologically and biomedically important antioxidants at which we are studying. In addition, $pK_{a1} = 3.74 \pm 0.05$ at 25.0°C and 1.0 M ionic strength for IAA has been determined in this work.

## Data Availability

All the data supporting the results are included in the manuscript.

## Conflicts of Interest

The authors declare that they have no conflicts of interest.

## Acknowledgments

Financial support of this work by grants from the Critical R&D Plans of Shandong Province (Major Scientific Innovation Projects, 2019JZZY010516) and from a setup fund of Zaozhuang University (1020717) is gratefully acknowledged.

## References

[1] S. K. Chang, A. Ismail, and Z. A. M. Daud, "Ascorbic acid: properties, determination and uses," *Encyclopedia of Food and Health*, pp. 275–284, 2016.

[2] B. Gómez Ruiz, S. Roux, F. Courtois, and C. Bonazzi, "Spectrophotometric method for fast quantification of ascorbic acid and dehydroascorbic acid in simple matrix for kinetics measurements," *Food Chemistry*, vol. 211, pp. 583–589, 2016.

[3] L. Ferrada, R. Magdalena, M. J. Barahona et al., "Two distinct faces of vitamin C: AA vs. DHA," *Antioxidants*, vol. 10, no. 2, p. 215, 2021.

[4] K. Zhang, S. Lv, Z. Lin, M. Li, and D. Tang, "Bio-bar-code-based photoelectrochemical immunoassay for sensitive detection of prostate-specific antigen using rolling circle amplification and enzymatic biocatalytic precipitation," *Biosensors and Bioelectronics*, vol. 101, pp. 159–166, 2018.

[5] Z. Yu, L. Huang, J. Chen, Y. Tang, B. Xia, and D. Tang, "Full-spectrum responsive photoelectrochemical immunoassay based on $\beta$-In2S3@carbon dot nanoflowers," *Electrochimica Acta*, vol. 332, Article ID 135473, 2020.

[6] K. Zhang, S. Lv, Q. Zhou, and D. Tang, "CoOOH nanosheets-coated g-C3N4/CuInS2 nanohybrids for photoelectrochemical biosensor of carcinoembryonic antigen coupling hybridization chain reaction with etching reaction," *Sensors and Actuators B: Chemical*, vol. 307, Article ID 127631, 2020.

[7] S. J. Padayatty, A. Katz, Y. Wang et al., "Vitamin C as an antioxidant: evaluation of its role in disease prevention," *Journal of the American College of Nutrition*, vol. 22, no. 1, pp. 18–35, 2003.

[8] A. M. Meščić Macan, T. G. Gazivoda Kraljević, and S. Raić-Malić, "Therapeutic perspective of vitamin C and its derivatives," *Antioxidants*, vol. 8, no. 8, p. 247, 2019.

[9] A. Bendich, L. J. Machlin, O. Scandurra, G. W. Burton, and D. D. M. Wayner, "The antioxidant role of vitamin C," *Advances in Free Radical Biology & Medicine*, vol. 2, no. 2, pp. 419–444, 1986.

[10] J. Shen, P. T. Griffiths, S. J. Campbell, B. Utinger, M. Kalberer, and S. E. Paulson, "Ascorbate oxidation by iron, copper and reactive oxygen species: review, model development, and derivation of key rate constants," *Scientific Reports*, vol. 11, no. 1, p. 7417, 2021.

[11] S. Zapata and J.-P. Dufour, "Ascorbic, dehydroascorbic and isoascorbic acid simultaneous determination by reverse phase ion interaction HPLC," *Journal of Food Science*, vol. 17, no. 12, pp. 506–511, 1992.

[12] B. L. Ling, W. R. G. Baeyens, P. van Acker, and C. Dewaele, "Determination of ascorbic acid and isoascorbic acid by capillary zone electrophoresis: application to fruit juices and to a pharmaceutical formulation," *Journal of Pharmaceutical and Bioanalytical Analysis*, vol. 10, no. 10-12, pp. 717–721, 1992.

[13] W. A. Behrens and R. Madère, "Ascorbic acid, isoascorbic acid, dehydroascorbic acid, and dehydroisoascorbic acid in selected food products," *Journal of Food Composition and Analysis*, vol. 7, no. 3, pp. 158–170, 1994.

[14] M. A. Kall and C. Andersen, "Improved method for simultaneous determination of ascorbic acid and dehydroascorbic acid, isoascorbic acid and dehydroisoascorbic acid in food and biological samples," *Journal of Chromatography B: Biomedical Sciences and Applications*, vol. 730, no. 1, pp. 101–111, 1999.

[15] Y. Zhao, H. Yuan, X. Zhang, and J. Yang, "A stimuli-responsive fluorescence platform for simultaneous determination of D-isoascorbic acid and tartaric acid based on Maillard reaction product," *Spectrochimica Acta Part A: Molecular and Biomolecular Spectroscopy*, vol. 196, pp. 1–6, 2018.

[16] Y.-H. P. Hsieh and Y. P. Hsieh, "Kinetics of Fe(III) reduction by ascorbic acid in aqueous solutions," *Journal of Agricultural and Food Chemistry*, vol. 48, no. 5, pp. 1569–1573, 2000.

[17] J. Dong, Y. Ren, S. Huo et al., "Reduction of ormaplatin and *cis*-diamminetetrachloroplatinum(IV) by ascorbic acid and dominant thiols in human plasma: kinetic and mechanistic analyses," *Dalton Transactions*, vol. 45, no. 28, pp. 11326–11337, 2016.

[18] Q. Wang, W.-L. Man, W. W. Y. Lam, and T.-C. Lau, "Oxidation of ascorbic acid by a (salen)ruthenium(vi) nitrido complex in aqueous solution," *Chemical Communications*, vol. 50, no. 99, pp. 15799–15802, 2014.

[19] M. Kröger-Ohlsen and L. H. Skibsted, "Kinetics and mechanism of reduction of ferrylmyoglobin by ascorbate and D-isoascorbate," *Journal of Agricultural and Food Chemistry*, vol. 45, no. 3, pp. 668–676, 1997.

[20] J. Dong, Y. Ren, S. Sun et al., "Kinetics and mechanism of oxidation of the anti-tubercular prodrug isoniazid and its analog by iridium(iv) as models for biological redox systems," *Dalton Transactions*, vol. 46, no. 26, pp. 8377–8386, 2017.

[21] C. Nan, J. Dong, H. Tian et al., "Oxidations of hydrazine and substituted hydrazines by hexachloroiridate(IV) in aqueous solution: kinetic and mechanistic analyses," *Journal of Molecular Liquids*, vol. 256, pp. 489–496, 2018.

[22] H. Yao, H. Tian, L. Xu et al., "Kinetic and mechanistic analysis of oxidation of 2-furoic hydrazide by hexachloroirradate(IV) in a wide pH range," *Transition Metal Chemistry*, vol. 44, no. 8, pp. 771–777, 2019.

[23] M. J. Dinsmore and J. S. Lee, "Hexachloroiridate(IV) as a redox probe for the electrochemical discrimination of B-DNA and M-DNA monolayers on gold," *Journal of Electroanalytical Chemistry*, vol. 617, no. 1, pp. 71–77, 2008.

[24] E. Kim, T. E. Winkler, C. Kitchen et al., "Redox probing for chemical information of oxidative stress," *Analytical Chemistry*, vol. 89, no. 3, pp. 1583–1592, 2017.

[25] E. Pelizzetti, E. Mentasti, and E. Pramauro, "Outer-sphere oxidation of ascorbic acid," *Inorganic Chemistry*, vol. 17, no. 5, pp. 1181–1186, 1978.

[26] W. D. Drury and J. M. DeKorte, "Specific-cation medium effects in the oxidation of ascorbic acid by hexachloroiridate(IV) and hexabromoiridate(IV)," *Inorganic Chemistry*, vol. 22, no. 1, pp. 121–125, 1983.

[27] M. Kimura, M. Yamamoto, and S. Yamabe, "Kinetics and mechanism of the oxidation ofL-ascorbic acid by tris(oxalato) cobaltate(III) and tris(1,10-phenanthroline)iron(III) complexes in aqueous solution," *Journal of the Chemical Society, Dalton Transactions*, vol. 2, no. 2, pp. 423–427, 1982.

[28] Y. Liu, H. Tian, L. Xu et al., "Investigations of the kinetics and mechanism of reduction of a carboplatin Pt(IV) prodrug by the major small-molecule reductants in human plasma," *International Journal of Molecular Sciences*, vol. 20, no. 22, p. 5660, 2019.

[29] Y. Xia, H. Tian, Y. Li et al., "Kinetic analysis of the reduction processes of a cisplatin Pt(IV) prodrug by Mesna, thioglycolic acid and thiolactic acid," *Journal of Chemistry*, vol. 2020, Article ID 5868174, 12 pages, 2020.

[30] X. Zhang, "Oxidations of benzhydrazide and phenylacetic hydrazide by hexachloroiridate(IV): reaction mechanism and structure-reactivity relationship," *Molecules*, vol. 25, no. 2, p. 308, 2020.

[31] C. Liu, L. Xu, H. Tian, H. Yao, L. I. Elding, and T. Shi, "Kinetics and mechanism for reduction of Pt(IV) anticancer model compounds by Se-methyl L-selenocysteine. Comparison with L-selenomethionine," *Journal of Molecular Liquids*, vol. 271, pp. 838–843, 2018.

[32] D. H. Macartney and A. McAuley, "The outer-sphere oxidation of ascorbic acid by the thioureapentacyanoferrate(III) ion," *Canadian Journal of Chemistry*, vol. 59, no. 1, pp. 132–137, 1981.

[33] S. Yamabe, N. Tsuchida, S. Yamazaki, and S. Sakaki, "Frontier orbitals and transition states in the oxidation and degradation ofl-ascorbic acid: a DFT study," *Organic and Biomolecular Chemistry*, vol. 13, no. 13, pp. 4002–4015, 2015.

[34] S. Huo, J. Dong, C. Song et al., "Characterization of the reaction products, kinetics and mechanism of oxidation of the drug captopril by platinum(IV) complexes," *RSC Advances*, vol. 4, no. 15, pp. 7402–7409, 2014.

[35] J. H. Espenson, *Chemical Kinetics and Reaction Mechanisms*, McGraw-Hill, New York, NY, USA, 2nd edition, 1995.

[36] J. Dong, S. Huo, S. Shen, J. Xu, T. Shi, and L. I. Elding, "Reactivity of the glutathione species towards the reduction of ormaplatin (or tetraplatin)," *Bioorganic & Medicinal Chemistry Letters*, vol. 26, no. 17, pp. 4261–4266, 2016.